Photoconductance oscillations in a two-dimensional quantum point contact

Anna Grincwajg,* L.Y. Gorelik,† V.Z. Kleiner,‡ and R.I. Shekhter
Department of Applied Physics, Chalmers University of Technology and Göteborg University, S-412 96 Göteborg, Sweden
(Received 29 March 1995)

We have calculated the photoconductance of a quantum point contact subject to a high-frequency electromagnetic field. We find very pronounced steplike oscillations of the photoconductance as a function of gate voltage. The absorption of the electromagnetic field, which is polarized in the transverse direction, is due to transitions between different modes of the quantum point contact. A transition between a propagating and a nonpropagating mode results effectively in a backscattering process, and gives a negative or positive contribution to the current, depending on the gate voltage. When the number of propagating modes through the point contact exceeds a cutoff value, the photoconductance disappears. The cutoff value depends on the frequency of the electromagnetic field. We also find that the oscillation amplitude increases with the number of propagating modes. As a result of the electron-photon interaction, the total quantized conductance acquires an additional step structure.

I. INTRODUCTION

Ballistic transport in two-dimensional electron systems has been very intensely studied during recent years. A particular system that has received much attention is the quantum point contact (QPC).[1] This structure is fabricated by putting a split gate on top of a GaAs heterostructure, thereby creating a narrow constriction in the two-dimensional electron gas. Since the electrons do not experience any collisions, the electron motion through the point contact is analogous to the propagation of an electromagnetic field through a waveguide. The width of the constriction, which is of the same order as the Fermi wavelength, is controlled by the gate voltage and governs the number of propagating modes.

The present work investigates the influence of a high-frequency electromagnetic field on the electric current through a quantum point contact. Despite the fact that transport properties have been thoroughly investigated for QPC systems, both experimentally[2–4] and theoretically,[5,6] this particular aspect has not so far received much attention.[7]

A closely related issue, optical absorption of a high-frequency field in a quantum point contact, has been studied by the present authors in an earlier work.[8] It was found that the optical absorption gives rise to a distinct spectrum, thus optical point contact spectroscopy is possible and can be used to characterize the laterally confining potential. The shape of this potential is still an open question, which makes a spectroscopy of this kind interesting. However, in a direct measurement of the absorption one is restricted by the fact that the volume of the point contact is much smaller than the total volume of the electromagnetic resonator. A very high quality factor of the resonator is therefore of crucial importance for such an experiment. The electric current, on the other hand, is more favorable to measure since in this case the observable quantity is located in the same small region in space where the absorption takes place. The photoconductance of a double quantum point contact has been investigated by the present authors in another work,[9] where it was shown that interference effects due to inelastic electron-photon scattering are possible.

It may not be evident that an electromagnetic field will at all affect the current through a quantum point contact. Since the photon momentum is much smaller than the electron momentum the photons cannot in a direct way backscatter electrons. However, as was shown in Ref. 7, the absorption of photons in a quantum point contact indirectly results in backscattering of electrons.

This fact can be explained as follows: In an adiabatic geometry, which is smooth on the scale of the Fermi wavelength, the longitudinal and transverse motion of electrons can be separated in the Schrödinger equation.[5] The transverse energy will then play the role of a potential for the one-dimensional longitudinal motion. Depending on whether the total energy of a given electronic state (mode) is larger or smaller than this potential barrier, it is a propagating or nonpropagating (reflecting) state. The absorption of the electromagnetic field, polarized in the transverse direction, is due to electron transitions between different modes in the system. If a transition between a propagating and a reflecting mode takes place it will effectively result in a backscattering process. This photon-induced backscattering gives rise to negative or positive photoconductance depending on the gate controlled width of the point contact. Therefore, the photoconductance will oscillate as a function of gate voltage.

II. FORMULATION OF THE PROBLEM

Our aim is to calculate the current through the microconstriction under the influence of a high-frequency electromagnetic field. The model geometry of the microconstriction is shown in Fig. 1. The width $D(x)$ varies smoothly on the scale of the Fermi wavelength, allowing

0163-1829/95/52(16)/12168(11)/$06.00

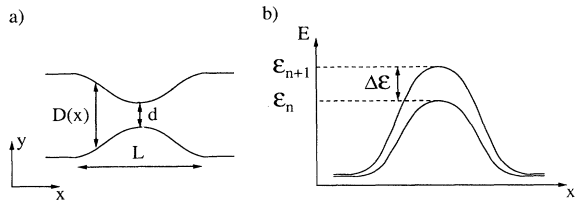

FIG. 1. (a) Geometry of the microconstriction. The width is denoted by $D(x)$, the narrowest width by d, and the effective length by L. (b) The corresponding transverse energies of modes n and $n+1$, as a function of x. The difference between the peak values is denoted by $\Delta\mathcal{E}$. If the initial state of the transition, mode n, is a nonpropagating state, the final-state mode $n+1$ will also be nonpropagating. On the other hand, if the initial state is propagating, the final state may be propagating or nonpropagating depending on the value of the longitudinal energy at $x=0$. See text for detailed explanation.

us to treat the problem in the adiabatic approximation. The high-frequency field, polarized in the y direction, induces transitions between the transverse states. The longitudinal momentum is conserved in the absorption process and therefore the photon energy $\hbar\omega$, where ω is the frequency of the field, must be equal to the energy difference between the transverse states. Since the electromagnetic field cannot change the direction of the electron propagation we can treat electrons coming from each side independently. In our calculations we will use the interaction representation. The total current $J^{\rm tot}$ through the point contact is calculated as

$$J^{\rm tot}=\mathrm{Tr}\{\hat{\rho}(t)\hat{J}\}, \tag{1}$$

where $\hat{\rho}(t)$ is the density operator and $\hat{J}$ is the current operator. The equation of motion for the density operator is

$$i\hbar\frac{\partial\hat{\rho}(t)}{\partial t}=[\hat{\rho}(t),\hat{H}(t)], \tag{2}$$

where the Hamiltonian of our system can be written as a sum of two parts:

$$\hat{H}=\hat{H}_{\rm el}+\hat{H}_{\rm int}. \tag{3}$$

We can express the current correction J to second order in the electron-photon coupling as

$$J=-\mathrm{Tr}\left\{\frac{\hat{\rho}_0}{\hbar^2}\int_{-\infty}^{t}dt'\times\int_{-\infty}^{t'}dt''[\hat{H}_{\rm int}(t''),[\hat{H}_{\rm int}(t'),\hat{J}]]\right\}, \tag{4}$$

$$\hat{J}=\frac{e}{2m^*}[\hat{p}\delta(\hat{x}-x_0)+\delta(\hat{x}-x_0)\hat{p}], \tag{5}$$

where $\hat{\rho}_0=\hat{\rho}(-\infty)$ and x_0 is the observation point. Keeping only the dipole term of the electron-photon interaction[10] the interaction part of the Hamiltonian can be expressed as

$$\hat{H}_{\rm int}=\sum_{\alpha\beta}A_{\alpha\beta}c_\alpha^\dagger c_\beta. \tag{6}$$

Here we sum over the states α and β and the operators $c_\alpha^\dagger$ and c_α are creation and annihilation operators for electrons in state α. The matrix element $A_{\alpha\beta}$ is of the form

$$A_{\alpha\beta}=-\frac{e\tilde{E}}{m^*\omega}\langle\alpha|\hat{p}_y|\beta\rangle, \tag{7}$$

$$\tilde{E}=\tilde{E}(t)=\frac{E}{2}(e^{i\omega t}+e^{-i\omega t}), \tag{8}$$

where the time-dependent electromagnetic field $\tilde{E}$ with frequency ω is polarized in the y direction, $\hat{p}_y$ is the y component of the electron momentum operator, and e and m^* are the electron charge and effective mass.

Evaluation of the time average of the current correction yields, written in operator form,

$$J=\sum_\alpha f_\alpha\{\langle\alpha|\hat{A}G^-(E_\alpha\pm\hbar\omega)\hat{J}G^+(E_\alpha\pm\hbar\omega)\hat{A}|\alpha\rangle+2\,\mathrm{Re}\langle\alpha|\hat{A}G^-(E_\alpha\pm\hbar\omega)\hat{A}G^-(E_\alpha)\hat{J}|\alpha\rangle\}, \tag{9}$$

where f_α is the distribution function and E_α is the total energy of an electron in the state α. The function $G^\pm(E)$ is the single-particle Green's function for an electronic state of energy E in the microconstriction,

$$G^\pm(E)=\frac{1}{E-\hat{H}_{\rm el}\pm i\delta}. \tag{10}$$

In the following section we will explicitly calculate the matrix element $A_{\alpha\beta}$ and the resulting photoconductance.

III. CALCULATION OF THE PHOTOCONDUCTANCE

The starting point here is the evaluation of the current correction J. The calculation is carried out in detail in Appendices A and B. Taking the applied voltage to be small, the photoconductance is found to be[11]

$$G^{\rm ph}=\frac{2\pi e^2}{\hbar}\sum_{\alpha\beta}\frac{\partial f_\alpha^0}{\partial\mu}[|\langle\beta_\rightarrow|\hat{A}|\alpha_{\leftrightarrow}\rangle|^2\delta(E_\alpha-E_\beta-\hbar\omega)-|\langle\alpha_\rightarrow|\hat{A}|\beta_{\leftrightarrow}\rangle|^2\delta(E_\alpha-E_\beta+\hbar\omega)], \tag{11}$$

where f_α^0 is the equilibrium electron distribution function and μ is the chemical potential. The voltage is applied so that the current flows from left to right. We have here introduced an arrow notation in the states $|\alpha_\rightarrow\rangle$ and $|\alpha_{\leftrightarrow}\rangle$. The arrows refer to propagating and reflecting modes, respectively, and also indicate that all the states occurring in the above expression are incident from the left.

Before we proceed any further, let us first analyze the expression (11). The physical meaning is quite straightforward. First of all, only transitions between a prop-

agating and a nonpropagating mode can contribute to the photoconductance. A transition where both modes are propagating or nonpropagating does obviously not change the current. Further, because all states below the Fermi level are occupied (at zero temperature) only absorption processes are possible.

The meaning of the two terms in (11), which have different signs, can be explained as follows. When applying a voltage V, driving the current from left to right, the chemical potential is increased by $eV/2$ at the left side and decreased by $eV/2$ at the right side (we assume a symmetric voltage drop). The change in chemical potential makes two types of absorption processes A and B possible, which are schematically shown in Fig. 2. Both these transitions result in a decrease of current, but since transition B is connected to the left-moving electrons, it gives a positive contribution to the photoconductance, while transition A, which is connected to the right-moving electrons, gives a negative contribution.

We wish to point out that the photoconductance in Eq. (11) contains only transitions from a propagating to a nonpropagating state, not the opposite case. The reason is that the transition from a nonpropagating to a propagating state is forbidden in the absorption case. It follows from the conservation of energy and longitudinal momentum as explained below.

Consider Fig. 1(b), where the transverse energies of modes n and $n+1$ are shown as a function of x. The difference between the peak values $\mathcal{E}_n$ and $\mathcal{E}_{n+1}$ is denoted by $\Delta\mathcal{E}$. Suppose now that the initial state, mode n, is a nonpropagating state. This can be expressed through the condition $E_n < \mathcal{E}_n$, where E_n is the total energy of the state. The total energy of the final state, mode $n+1$, is then

$$E_{n+1} = E_n + \hbar\omega < \mathcal{E}_n + \hbar\omega = \mathcal{E}_{n+1} - (\Delta\mathcal{E} - \hbar\omega). \quad (12)$$

Since we always have that $\Delta\mathcal{E} > \hbar\omega$ (otherwise there cannot be a transition between the modes being considered) we find that $E_{n+1} < \mathcal{E}_{n+1}$, which means that also the final state is nonpropagating. It can easily be shown in a similar way that if the initial state is propagating, the final state will be nonpropagating if the longitudinal energy at $x = 0$ is smaller than $\Delta\mathcal{E} - \hbar\omega$. The latter is the only type of transition that will change the current, and it is this type that occurs in Eq. (11) for the photoconductance.

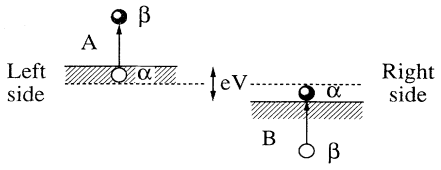

FIG. 2. When applying a voltage V across the irradiated point contact, driving the current from left to right, two types of transitions A and B become possible. Transition A at the left side, which involves right-moving states, gives a negative contribution to the photoconductance while transition B at the right side, which involves left-moving states, gives a positive contribution. These two contributions result in steplike oscillations of the photoconductance. The quantum numbers α and β label the states appearing in Eq. (11) for the photoconductance.

To obtain the photoconductance we must calculate the matrix element $A_{\alpha\beta}$. The state $|\alpha\rangle$ can quite generally be characterized by the mode number n, the longitudinal electron momentum p far away from the microconstriction, and a sign index σ as follows:

$$|\alpha\rangle = |n, p, \sigma\rangle, \quad n = 0, 1, 2, 3\ldots, \quad \sigma = \pm 1. \quad (13)$$

Here the sign index σ denotes which side of the microconstriction the electron originates from. In the calculation of the matrix element we will only deal with states originating from the left side (see above), i.e., $\sigma = +1$. The adiabatic microconstriction geometry allows us to separate the electron wave function into one longitudinal and one transverse part. Taking the laterally confining potential to be of the parabolic type,[12] the transverse wave function can be expressed in terms of Hermite polynomials and the corresponding transverse energy of mode n is

$$E_n(x) = \frac{\hbar^2}{2m^*}\frac{2n+1}{D^2(x)}, \quad (14)$$

where $D(x)$ is the width of the microconstriction. The longitudinal wave functions for propagating and reflecting modes, respectively, are taken as

$$\Psi_{\alpha\rightarrow}(x) = \sqrt{\frac{p_n(-\infty)}{2\pi\hbar p_n(x)}}\exp\left(\frac{i}{\hbar}\int^x dx' p_n(x')\right),$$

propagating state, (15)

$$\Psi_{\beta\leftarrow}(x) = \sqrt{\frac{p_n(-\infty)}{\pi\hbar p_n(x)}}\sin\left(\frac{1}{\hbar}\int_{x_m}^x dx' p_m(x')\right),$$

reflecting state, (16)

$$p_n(x) = \sqrt{2m^*[E_\alpha - E_n(x)]}, \quad (17)$$

where x_m is the turning point for the reflecting state. When evaluating the x integral in the matrix elements appearing in (11) we use the stationary phase approximation. This is not a trivial calculation, however. The difficulties arise because the wave functions (15) and (16) are rapidly oscillating functions of x. A detailed analysis of this problem was made by Landau,[13] who reduced the calculation of the x integral to the evaluation of a contour integral in the complex plane. There are several contributions to this contour integral. The dominant contributions come from the stationary phase points x^*, which are located on the real axis at points where the contour crosses the real axis. These are points where the transition between different electron states occurs in such a way

that the longitudinal momentum is conserved. Hence

$$p_n(x^*) = p_m(x^*). \tag{18}$$

Other contributions come from points where the effective potential $E_n(x)$ is singular in the complex plane. These contributions correspond to processes where the momentum is not exactly conserved due to the adiabatic variation of the potential energy. It is easy to show that for transitions between propagating and nonpropagating modes these contributions are proportional to $\exp -L/d$, where L and d are the length and width of the microconstriction, and hence exponentially small. Therefore, only the stationary points give non-negligible contributions to the photon induced matrix elements. According to Landau[13] there are no contributions from the classical turning points to the quasiclassical matrix elements.

Here we wish to point out that the quasiclassical matrix elements discussed above were calculated in Ref. 14, where the photoconductance of an adiabatic point contact was considered. A numerical calculation based on uncontrollable approximations brings the authors to the incorrect conclusion that photon-assisted transport processes occur mainly near the classical turning points. As a result the photoconductance calculation based on this assumption seems to be incorrect. Our result for the matrix element is[8]

$$A_{\alpha\beta} = \frac{eE}{2m^*\omega}\sqrt{\frac{k_n(-\infty)k_m(-\infty)}{2\pi k_n(x^*)}}\sqrt{\left|\frac{D(x^*)}{D'(x^*)}\right|} \times\{\sqrt{n+1}\delta_{m,n+1} - \sqrt{n}\delta_{m,n-1}\}. \tag{19}$$

We are now ready to write down the final expression for the photoconductance. Replacing the derivative of the Fermi function in Eq. (11) by a δ function, which is reasonable for sufficiently low temperatures, and introducing the dimensionless frequency $\Omega = \hbar\omega/E_F$ where E_F is the Fermi energy we obtain

$$G^{\rm ph} = \frac{2e^2}{h}\left(\frac{eE}{\hbar\omega}\right)^2\frac{\pi}{4}\sum_n \frac{\Theta[1-\Omega(n+1/2)]}{k_F\sqrt{1-\Omega(n+1/2)}}\left|\frac{D(x^*)}{D'(x^*)}\right| \times\{n\Theta[(2n+1) - k_F^2d^2]\Theta[k_F^2d^2(1-\Omega) -(2n-1)] - (n+1)\Theta[k_F^2d^2 - (2n+1)] \times\Theta[2n+3-k_F^2d^2(1+\Omega)]\}. \tag{20}$$

The step function $\Theta[1-\Omega(n+1/2)]$ expresses the condition that the stationary point x^* must be in the classically allowed region for the electrons, a condition imposed by the existence of turning points. The step functions within the curly brackets express the conditions for the modes being propagating or nonpropagating. Depending on the narrowest width d of the microconstriction, one, both, or none of these step functions give a contribution, which results in steplike oscillations of the photoconductance as a function of d. These oscillations will be analyzed in detail in the next section.

In order to have any absorption at all, we also have the condition that the photon energy must be smaller than the maximum difference between the transverse energy levels

$$\Omega < \frac{2}{k_F^2d^2}. \tag{21}$$

Expression (20) for the photoconductance is valid for a general microconstriction geometry. In the next section we will consider a specific model geometry and analyze the resulting features of the photoconductance and the total conductance.

IV. RESULTS AND DISCUSSION

For a detailed numerical analysis we use a model geometry of the microconstriction where the width $D(x)$ of the narrow part has an exponential x dependence

$$D(x) = d\exp(x^2/2L^2). \tag{22}$$

Here d is the narrowest width and L is the effective length of the microconstriction [see Fig. 1(a)]. However, the results are not sensible to the particular choice of geometry, as long as it is adiabatically smooth on the scale of the Fermi wavelength.[8] The geometrical factor $|D(x^*)/D'(x^*)|$ is then

$$\left|\frac{D(x^*)}{D'(x^*)}\right| = \frac{L}{\sqrt{\ln(2/\Omega k_F^2d^2)}}. \tag{23}$$

The condition (21) that the photon energy must be smaller than the maximum difference between the transverse energy levels, prevents the denominator of the geometry factor to be zero.

Our expression for the photoconductance depends on a number of parameters. In all calculations we use the Fermi temperature $T_F = 200$ K and the length of the microconstriction $L = 1$ μm. The photoconductance and total conductance are studied as a function of microconstriction width d for different choices of electromagnetic field amplitude E and frequency ω.

In Fig. 3 the photoconductance is shown as a function of microconstriction width for two different amplitudes and frequencies of the electromagnetic field: (a) $E = 80$ V/cm, $\Omega = 0.19$ (which corresponds to $\omega = 7.8\times10^{11}$ s^{-1}) and (b) E = 140 V/cm, $\Omega = 0.35$ (which corresponds to $\omega = 1.4\times10^{12}$ s^{-1}). The photoconductance exhibits very pronounced steplike oscillations up to a cutoff value of the microstructure width. The cutoff value depends on frequency, and it is seen in Fig. 3(a) that five propagating modes give a contribution while in Fig. 3(b) there is a contribution from three propagating modes only. The oscillations are a result of the condition that the initial state of the transition must be propagating and the final state nonpropagating. Depending on the width of the microstructure, the photoconductance in Eq. (20) is given by one, both, or none of the two terms with opposite sign.

The contributions from the positive and negative term on a single step with step number n are shown schemati-

cally in the inset of Fig. 3. The amplitudes of both terms are in this simplified picture taken to be equal and normalized to unity. The width of the step is also unity here. The widths of the negative and positive contributions are denoted by Δ_- and Δ_+, respectively, and they depend on step number and frequency as

$$\Delta_- = \frac{1-\Omega(n+1/2)}{1+\Omega}\Theta[1-\Omega(n+1/2)], \tag{24}$$

$$\Delta_+ = \frac{1-\Omega(n+3/2)}{1-\Omega}\Theta[1-\Omega(n+3/2)]. \tag{25}$$

Note that on a single step with number n the mode with number n gives the contribution Δ_-, and the mode with number $n+1$ gives the contribution Δ_+. We see that the widths Δ_- and Δ_+ decrease with increasing step number and finally become zero. This leads to the cutoff and also explains why the photoconductance "peaks" get narrower as the step number increases.

The two contributions Δ_- and Δ_+ overlap each other when

$$\Omega < \frac{1}{2(n+1)}. \tag{26}$$

For low step numbers the overlap region is large, but as n increases the overlap region decreases and finally becomes zero. Since the two terms have slightly different amplitudes, because of the factor $1/k_F\sqrt{1-\Omega(n+1/2)}$ [see Eq. (20)], they do not overlap completely.

The amplitude of the oscillations increases with microconstriction width. The largest amplitude is found for the highest mode numbers, since the denominators in Eq. (20) decrease with increasing mode numbers.

In Fig. 4 the total conductance is shown as a function of microstructure width. The dimensionless frequency is $\Omega = 0.19$ and the amplitude of the electromagnetic field is E= 80 V/cm, the same values as in Fig. 3(a) (solid line). The dotted line shows the conductance in the absence of an electromagnetic field. It is seen that the electron-photon interaction leads to an additional step structure of the conductance, becoming more pronounced for higher steps. The narrowing of the photoconductance oscillation "peaks" with increasing step number is a striking feature, which is in contrast to what one could expect for these systems. Normally a smearing of the fine structure occurs as the width of the microconstriction increases.

We wish to point out that all the above considerations are based on the single-photon approximation; i.e., resonance effects such as Rabi oscillations are not taken into account. The single-photon approximation is valid if the time t_0 spent by an electron at resonance is less than the characteristic time of resonant photon-assisted intermode transitions. The latter is equal to the inverse of the so-called Rabi frequency $\omega_R = A_{\alpha\beta}/\hbar$, which determines the dynamics of a two-level system in a resonant field. The time spent at resonance can be determined from the uncertainty principle; since the electron spends a finite time t_0 near resonance its energy is uncertain to within $\delta E = \hbar/t_0$. On the other hand, the energy difference between the two resonating states α and β changes with time as the electron moves. During

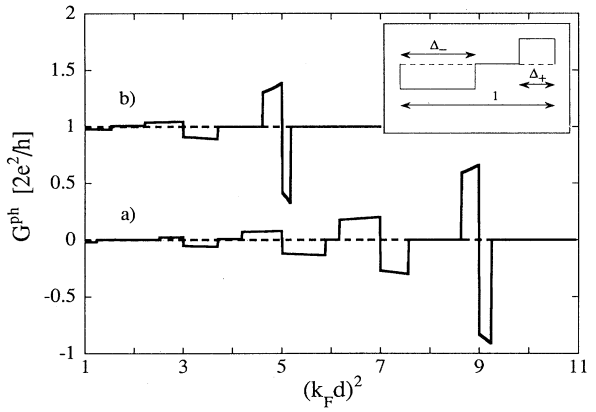

FIG. 3. Photoconductance as a function of the dimensionless parameter $(k_Fd)^2$ where d is the narrowest microstructure width. The two graphs — vertically offset for clarity — correspond to two different amplitudes and frequencies of the electromagnetic field: (a) E= 80 V/cm, $\omega = 7.8 \times 10^{11}$ s^{-1} and (b) E= 140 V/cm, $\omega = 1.4 \times 10^{12}$ s^{-1}. The photoconductance exhibits very pronounced steplike oscillations up to a cutoff value of the number of propagating modes. The cutoff value depends on the frequency ω. In case (a) there is a contribution from five propagating modes while in case (b) three propagating modes contribute. The inset shows the normalized contributions from the positive and negative terms of the photoconductance, shown on a single step. The widths of the negative and positive contributions are denoted by Δ_- and Δ_+, respectively, and they depend on step number n and dimensionless frequency Ω (see text).

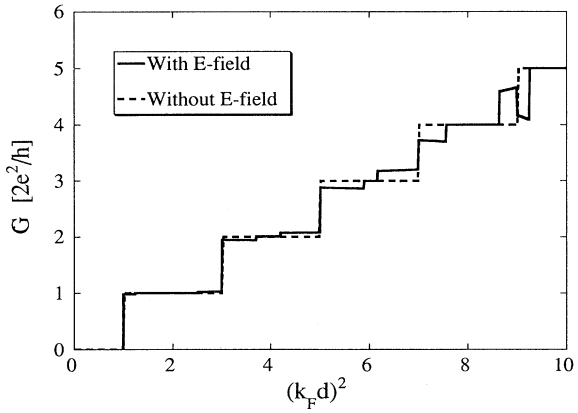

FIG. 4. Conductance as a function of the dimensionless parameter $(k_Fd)^2$. The amplitude and frequency of the electromagnetic field are the same as in Fig. 3(a), E = 80 V/cm and $\omega = 7.8 \times 10^{11}$ s^{-1} (solid line). The dotted line is the conductance in the absence of an electromagnetic field. It is seen that the electron-photon interaction leads to an additional step structure of the conductance, becoming more pronounced for higher steps.

the time t_0, the energy difference shifts from the value $E_{\alpha\beta} \equiv \hbar\omega$ corresponding to an exact resonance by an amount $\Delta E_{\alpha\beta} = \{E_n[x^* - v(x^*)t_0] - E_m[x^* - v(x^*)t_0]\}$. [Here $v(x^*)$ is the electron velocity at the resonance point.] The time t_0 can now be determined by equating δE and $\Delta E_{\alpha\beta}$. We find that $t_0 = [v(x^*)E'_{\alpha\beta}(x^*)/\hbar]^{-1/2}$. The single-photon approximation is therefore valid provided $A_{\alpha\beta}(x^*)/\sqrt{\hbar E'_{\alpha\beta}(x^*)v(x^*)} \ll 1$.

Using the definition of $E_n(x)$, we find that this criterion coincides with the criterion for the photon-induced step heights to be smaller than the conductance quantum $2e^2/h$. Using the above result the following restrictions on the amplitude of the electromagnetic field apply to the cases being considered above; (a) $E < 170$ V/cm, $\Omega = 0.19$; (b) $E < 190$ V/cm, $\Omega = 0.35$.

Another restriction on the amplitude of the electromagnetic field comes from the necessity to avoid heating of the electron gas in the source and drain regions. Heating results in a smearing of the photon-induced step structure in the conductance and gives rise to a bolometric effect rather than to photon-assisted transport.[15] Here the thermal properties of the actual experimental device come into play and no general criterion can be given.

In conclusion we have calculated the photoconductance of a quantum point contact. It is found that the absorption of a high-frequency electromagnetic field, polarized in the transverse direction, results in steplike oscillations of the photoconductance as a function of gate voltage. The absorption is due to transitions between different transverse energy states (or modes) of the quantum point contact. The modes can be either propagating or nonpropagating, and we find that a transition between a propagating and a nonpropagating mode results effectively in a backscattering process. This backscattering will decrease or increase the current, depending on the width of the microconstriction. Therefore the photoconductance oscillates as a function of gate voltage.

As a result of these oscillations the total quantized conductance acquires an additional step structure. The oscillations survive up to a cutoff value of the number of propagating modes. The cutoff value depends on the frequency of the electromagnetic field, and decreases as the frequency increases. We also find that the oscillation peaks become narrower and higher as the number of propagating modes increases. Our estimates of the electromagnetic field strength and frequency needed to observe this effect indicate that experimental verification of our predictions should be possible with present technology.[16]

ACKNOWLEDGMENTS

This work was supported by the Swedish Royal Academy of Sciences (KVA) and the Natural Science Research Council (NFR). Two of us (L.G. and V.K.) acknowledge the hospitality of the Department of Applied Physics, CTH/GU. We gratefully acknowledge discussions with T. Claeson, D.K. Ferry, M. Jonson, E. Kollberg, and O.Vendik.

APPENDIX A

When calculating the current response to an electromagnetic field, the electronic state $|\alpha\rangle$ occurring in our expression (9) is for the case of zero field. It is convenient for our purposes to express this state in terms of the transition matrix T. The transition matrix will thus be used to describe the scattering produced by the microconstriction, since we can view the electronic motion as a scattering problem. The microconstriction of varying width plays the role of a scatterer, which acts as a perturbation to a channel of constant width.

For the adiabatically smooth geometry considered here, Fig. 1(a), we can separate the longitudinal and transverse electronic motion in the Schrödinger equation. We are then left with an x-dependent transverse energy $E_n(x)$ of the form (14) which acts as a scattering potential for the one-dimensional longitudinal motion. Far away from the microconstriction the width is constant and we denote the Hamiltonian in this region by H_0. The scattering potential $V(x)$ can then be expressed as $V(x) = E_n(x) - E_n(\infty)$. In other words, the Hamiltonian $H_{\rm el}$ [see Eq. (3)], which describes the electrons in the absence of an electromagnetic field, can be split into two parts:

$$H_{\rm el} = H_0 + V. \tag{A1}$$

The above equation defines our scattering problem. In the calculations we will make use of the functions $G_0^{\pm}$ and $G^{\pm}$, which are electron Green's functions connected to the Hamiltonians H_0 and $H_{\rm el}$, respectively, and are defined as follows,

$$G_0^{\pm}(E) = \frac{1}{E - \hat{H}_0 \pm i\delta}, \tag{A2}$$

$$G^{\pm}(E) = \frac{1}{E - \hat{H}_{\rm el} \pm i\delta}. \tag{A3}$$

As usual, the transition matrix $T^{\pm}$ is defined by the relationship

$$G^{\pm}(E) = G_0^{\pm}(E) + G_0^{\pm}(E)T^{\pm}(E)G_0^{\pm}(E), \tag{A4}$$

and can be expressed as a series expansion in the scattering potential V:

$$T^{\pm} = V + VG_0^{\pm}V + VG_0^{\pm}VG_0^{\pm}V + \cdots. \tag{A5}$$

Now, by using the transition matrix $T^{\pm}$, the electron state in the microconstriction, $|\Psi^{\pm}_{n,p,\sigma}\rangle$, can be expressed in terms of the unperturbed state $|\Phi_{n,p,\sigma}\rangle$ as

$$|\Psi^{\pm}_{n,p,\sigma}\rangle = |\Phi_{n,p,\sigma}\rangle + G_0^{\pm}(E)T^{\pm}(E)|\Phi_{n,p,\sigma}\rangle, \tag{A6}$$

$$n = 0, 1, 2, ..., \quad \sigma = \pm 1. \tag{A7}$$

Each state is here characterized by the discrete mode number n, the continuous momentum p far away from the microconstriction, and the sign index σ, which denotes whether the electron originates from the left ($\sigma = +1$) or right ($\sigma = -1$) side of the microconstriction. The total energy is here denoted by E, and is the sum of the

longitudinal and transverse energy:

$$E = \frac{p^2}{2m^*} + E_n(\infty). \tag{A8}$$

The unperturbed state $|\Phi_{n,p,\sigma}\rangle$ describes an electron moving in a channel of constant width, with Hamiltonian H_0. The $\pm$ sign in the superscript of the scattered state $|\Psi^{\pm}_{n,p,\sigma}\rangle$ denotes the retarded and advanced solution, respectively, so the "physical" state $|\alpha\rangle$ in our expression (9) corresponds to the state with the + sign,

$$|\alpha\rangle = |\Psi^{+}_{n,p,\sigma}\rangle. \tag{A9}$$

The summation over the state α corresponds to a summation over mode number n, sign σ, and an integration over momentum p:

$$\sum_{\alpha} = \sum_{n}\sum_{\sigma}\int_0^{\infty} dp. \tag{A10}$$

Now we are ready to treat Eq. (9). The current correction J consists of two terms that we denote J_1 and J_2:

$$J = J_1 + J_2, \tag{A11}$$

$$J_1 = \sum_{\alpha} f_\alpha \langle\alpha|\hat{A}G^{-}(\mathcal{E}_\alpha)\hat{J}G^{+}(\mathcal{E}_\alpha)\hat{A}|\alpha\rangle, \tag{A12}$$

$$J_2 = 2\sum_{\alpha} f_\alpha \mathrm{Re}\langle\alpha|\hat{A}G^{-}(\mathcal{E}_\alpha)\hat{A}G^{-}(E_\alpha)\hat{J}|\alpha\rangle, \tag{A13}$$

where we have introduced the energy $\mathcal{E}_\alpha = E_\alpha \pm \hbar\omega$. First, let us consider the term J_1. Using Eq. (A4) we can rewrite the matrix element in J_1 as

$$\langle\alpha|\hat{A}G^{-}(\mathcal{E}_\alpha)\hat{J}G^{+}(\mathcal{E}_\alpha)\hat{A}|\alpha\rangle = \langle\Psi^{+}_{n,p,\sigma}|\underbrace{\hat{A}[1+G_0^{-}(\mathcal{E}_\alpha)T^{-}]}_{\hat{\mathcal{A}}^{-}} G_0^{-}(\mathcal{E}_\alpha)\hat{J}G_0^{+}(\mathcal{E}_\alpha)\underbrace{[1+T^{+}G_0^{+}(\mathcal{E}_\alpha)]\hat{A}}_{\hat{\mathcal{A}}^{+}}|\Psi^{+}_{n,p,\sigma}\rangle, \tag{A14}$$

where we have introduced the operators $\hat{\mathcal{A}}^{+}$ and $\hat{\mathcal{A}}^{-}$. Now we will use the fact that the Green's functions $G_0^{+}(\mathcal{E}_\alpha)$ and $G_0^{-}(\mathcal{E}_\alpha)$ appearing immediately to the right and left of the current operator can be expressed as projection operators. This is possible only if the current operator $\hat{J}$ does not overlap with the operators $\hat{\mathcal{A}}^{+}$ and $\hat{\mathcal{A}}^{-}$ (which can also be expressed as $\hat{J}\hat{\mathcal{A}}^{\pm}=\hat{\mathcal{A}}^{\pm}\hat{J}=0$) and is shown in detail in Appendix B. The condition of no overlap is fulfilled in our case if we take the electromagnetic field to be nonzero only in the vicinity of the microconstriction while the current is to be calculated at a point x_0 far away from the microconstriction. The Green's function $G_0^{\pm}(\mathcal{E}_\alpha)$ can then be written as

$$G_0^{\pm}(\mathcal{E}_\alpha) = \mp 2\pi i \sum_{l,\sigma'} \delta_{\sigma',+1}\frac{m^*}{p'(\mathcal{E}_\alpha)}|\Phi_{l,p',\sigma'}\rangle\langle\Phi_{l,p',\sigma'}|, \tag{A15}$$

$$p'(\mathcal{E}_\alpha) = \sqrt{2m^*[\mathcal{E}_\alpha - E_l(\infty)]}, \tag{A16}$$

where E_l is the transverse energy of mode l. Inserting Eq. (A15) into Eq. (A14) and using the Lippmann-Schwinger equation in closed form

$$(1 + G_0^{\pm}T^{\pm})|\Phi\rangle = |\Psi^{\pm}\rangle, \tag{A17}$$

the operator in the matrix element (A14) is found to be

$$\hat{A}G^{-}(\mathcal{E}_\alpha)\hat{J}G^{+}(\mathcal{E}_\alpha)\hat{A} = 4\pi^2\sum_{l,\sigma'}\sum_{r,\sigma''}\delta_{\sigma',+1}\delta_{\sigma'',+1}\frac{m^{*2}}{p'(\mathcal{E}_\alpha)p''(\mathcal{E}_\alpha)}\hat{A}|\Psi^{-}_{l,p',\sigma'}\rangle\langle\Phi_{l,p',\sigma'}|\hat{J}|\Phi_{r,p'',\sigma''}\rangle\langle\Psi^{-}_{r,p'',\sigma''}|\hat{A}, \tag{A18}$$

$$p''(\mathcal{E}_\alpha) = \sqrt{2m^*[\mathcal{E}_\alpha - E_r(\infty)]}. \tag{A19}$$

The matrix element of the current operator in the above expression can now be evaluated as

$$\langle\Phi_{l,p',\sigma'}|\hat{J}|\Phi_{r,p'',\sigma''}\rangle = \frac{1}{2\pi\hbar}\frac{ep'(\mathcal{E}_\alpha)}{m^*}\delta_{lr}\delta_{\sigma',\sigma''}. \tag{A20}$$

Now we can obtain the following expression for J_1:

$$J_1 = \frac{2\pi e}{\hbar}\sum_{\alpha}\sum_{l,\sigma'}\delta_{\sigma',+1}f_\alpha\frac{m^*}{p'(\mathcal{E}_\alpha)}|\langle\Psi^{+}_{n,p,\sigma}|\hat{A}|\Psi^{-}_{l,p',\sigma'}\rangle|^2. \tag{A21}$$

It is convenient to separate J_1 into two parts:

$$J_1 = J_1^{\rightleftarrows} + J_1^{\Leftrightarrow}, \tag{A22}$$

$$J_1^{\rightleftarrows} = \frac{2\pi e}{\hbar}\sum_{\alpha}\sum_{l,\sigma'}\delta_{\sigma,+1}\delta_{\sigma',+1}(f_\alpha - f_{\tilde{\alpha}})\frac{m^*}{p'(\mathcal{E}_\alpha)}|\langle\Psi^{+}_{n,p,\sigma}|\hat{A}|\Psi^{-}_{l,p',\sigma'}\rangle|^2, \tag{A23}$$

$$J_1^{\Leftrightarrow} = \frac{2\pi e}{\hbar}\sum_{\alpha}\sum_{l,\sigma'}\delta_{\sigma,+1}\delta_{\sigma',+1}f_{\tilde{\alpha}}\frac{m^*}{p'(\mathcal{E}_\alpha)}\left(|\langle\Psi^{+}_{n,p,-\sigma}|\hat{A}|\Psi^{-}_{l,p',\sigma'}\rangle|^2 + |\langle\Psi^{+}_{n,p,\sigma}|\hat{A}|\Psi^{-}_{l,p',\sigma'}\rangle|^2\right). \tag{A24}$$

Here we have introduced the state $\tilde{\alpha}$ in the distribution function $f_{\tilde{\alpha}}$. The difference between the states $|\alpha\rangle$ and $|\tilde{\alpha}\rangle$ is that they have opposite signs of the index σ,

$$\alpha = \{n, p, \sigma\}, \tag{A25}$$

$$\tilde{\alpha} = \{n, p, -\sigma\}. \tag{A26}$$

Therefore, $\delta_{\sigma,+1} f_\alpha$ is the distribution function for electrons coming from the left side of the microconstriction and $\delta_{\sigma,+1} f_{\tilde{\alpha}}$ is the distribution function for electrons coming from the right side. We see that the term $J_1^{\Rightarrow}$ contains only states originating from the left side, while the term $J_1^{\Leftrightarrow}$ contains states originating from both sides.

Now let us turn our attention to J_2. The situation is somewhat different, since the matrix element does not have the same symmetry as in the case of J_1. However, we can treat the right part of the matrix element in the same way as we did for J_1, with the result

$$\hat{A}G^-(E_\alpha)\hat{J}|\Psi^+_{n,p,\sigma}\rangle = 2\pi i \sum_{l,\sigma'} \delta_{\sigma',+1} \frac{m^*}{p'(E_\alpha)} \hat{A}|\Psi^-_{l,p',\sigma'}\rangle\langle\Phi_{l,p',\sigma'}|\hat{J}|\Psi^+_{n,p,\sigma}\rangle. \tag{A27}$$

The next step is to evaluate the matrix element for the current operator in the above expression,

$$\begin{aligned}\langle\Phi_{l,p',\sigma'}|\hat{J}|\Psi^+_{n,p,\sigma}\rangle &= \langle\Phi_{l,p',\sigma'}|\hat{J}[1 + G_0^+(E_\alpha)T^+(E_\alpha)]|\Phi_{n,p,\sigma}\rangle \\ &= \frac{1}{2\pi\hbar}\frac{ep'}{m^*}\delta_{ln}\delta_{\sigma\sigma'} - 2\pi i \sum_{r,\sigma''} \delta_{\sigma'',+1}\frac{m^*}{p''}\langle\Phi_{l,p',\sigma'}|\hat{J}|\Phi_{r,p'',\sigma''}\rangle\langle\Phi_{r,p'',\sigma''}|T^+(E_\alpha)|\Phi_{n,p,\sigma}\rangle \\ &= \frac{1}{2\pi\hbar}\frac{ep'}{m^*}\left(\delta_{ln}\delta_{\sigma\sigma'} - 2\pi i\frac{m^*}{p'}\langle\Phi_{l,p',\sigma'}|T^+(E_\alpha)|\Phi_{n,p,\sigma}\rangle\right).\end{aligned} \tag{A28}$$

Inserting Eq. (A28) into Eq. (A27) and taking into account the following relationship:[17]

$$\langle\Psi^-_{l,p',\sigma'}|\Psi^+_{n,p,\sigma}\rangle = \delta_{ln}\delta_{\sigma\sigma'}\delta(p-p') - 2\pi i\delta\left[E_l(p') - E_n(p)\right]\langle\Phi_{l,p',\sigma'}|T^+|\Phi_{n,p,\sigma}\rangle \tag{A29}$$

we can express J_2 as

$$J_2 = \mathrm{Re}\left\{\frac{2ie}{\hbar}\sum_\alpha\sum_{l,\sigma'}\delta_{\sigma',+1}f_\alpha\int_0^\infty dp'\langle\Psi^+_{n,p,\sigma}|\underbrace{\hat{A}G^-(\mathcal{E}_\alpha)\hat{A}}_{\hat{\mathcal{B}}}|\Psi^-_{l,p',\sigma'}\rangle\langle\Psi^-_{l,p',\sigma'}|\Psi^+_{n,p,\sigma}\rangle\right\}. \tag{A30}$$

Now let us separate our expression for J_2 into two parts, in the same way as we did for J_1:

$$J_2 = J_2^{\Rightarrow} + J_2^{\Leftrightarrow}, \tag{A31}$$

$$J_2^{\Rightarrow} = -\frac{2e}{\hbar}\mathrm{Im}\left\{\sum_\alpha\sum_{l,\sigma'}\delta_{\sigma,+1}\delta_{\sigma',+1}(f_\alpha - f_{\tilde{\alpha}})\int_0^\infty dp'\langle\Psi^+_{n,p,\sigma}|\hat{\mathcal{B}}|\Psi^-_{l,p',\sigma'}\rangle\langle\Psi^-_{l,p',\sigma'}|\Psi^+_{n,p,\sigma}\rangle\right\}, \tag{A32}$$

$$\begin{aligned}J_2^{\Leftrightarrow} = -\frac{2e}{\hbar}\mathrm{Im}\Bigg\{&\sum_\alpha\sum_{l,\sigma'}\delta_{\sigma,+1}\delta_{\sigma',+1}f_{\tilde{\alpha}}\int_0^\infty dp'(\langle\Psi^+_{n,p,\sigma}|\hat{\mathcal{B}}|\Psi^-_{l,p',\sigma'}\rangle\langle\Psi^-_{l,p',\sigma'}|\Psi^+_{n,p,\sigma}\rangle \\ &+\langle\Psi^+_{n,p,-\sigma}|\hat{\mathcal{B}}|\Psi^-_{l,p',\sigma'}\rangle\langle\Psi^-_{l,p',\sigma'}|\Psi^+_{n,p,-\sigma}\rangle)\Bigg\}.\end{aligned} \tag{A33}$$

In analogy with J_1, the term $J_2^{\Rightarrow}$ contains only states originating from the left side, while the term $J_2^{\Leftrightarrow}$ contains states originating from both sides.

When summing up the terms in Eq. (A31) and Eq. (A22) to obtain the total current, we find that $J_1^{\Leftrightarrow}$ and $J_2^{\Leftrightarrow}$ cancel each other. The remaining terms $J_1^{\Rightarrow}$ and $J_2^{\Rightarrow}$ are proportional to $(f_\alpha - f_{\tilde{\alpha}})$, the difference between the distribution functions at the right and left side of the microconstriction, as is expected for the current.

The cancellation of the terms $J_1^{\Leftrightarrow}$ and $J_2^{\Leftrightarrow}$ is a consequence of the assumed geometrical symmetry of our microconstriction. A special case of an asymmetric geometry has been studied by Fedichkin, Ryzhii, and V'yurkov,[18] leading to a photovoltaic effect.

In our adiabatic geometry the term $J_2^{\Rightarrow}$ can be rewritten as

$$J_2^{\Rightarrow} = -\frac{2e}{\hbar}\mathrm{Im}\left\{\sum_\alpha \delta_{\sigma,+1}(f_\alpha - f_{\tilde{\alpha}})t_n\langle\Psi^+_{n,p,\sigma}|\hat{\mathcal{B}}|\Psi^-_{n,p,\sigma}\rangle\right\} \tag{A34}$$

$$= -\frac{2\pi e}{\hbar}\sum_{\alpha}\delta_{\sigma,+1}(f_\alpha - f_{\tilde{\alpha}})|t_n|\langle\Psi^+_{n,p,\sigma}|\hat{A}\delta(E_\alpha - \hat{H} \pm \hbar\omega)\hat{A}|\Psi^+_{n,p,\sigma}\rangle \tag{A35}$$

$$= -\frac{2\pi e}{\hbar}\sum_{\alpha}\sum_{\beta}\delta_{\sigma,+1}(f_\alpha - f_{\tilde{\alpha}})|t_n|\langle\Psi^+_{n,p,\sigma}|\hat{A}|\Psi^+_{l,p',\sigma'}\rangle\langle\Psi^+_{l,p',\sigma'}|\hat{A}|\Psi^+_{n,p,\sigma}\rangle\delta(E_\alpha - E_\beta \pm \hbar\omega). \tag{A36}$$

Here we have used the relations

$$\langle\Psi^-_{l,p',\sigma'}|\Psi^+_{n,p,\sigma}\rangle = t_n\delta_{ln}\delta_{\sigma'\sigma}\delta(p'-p) \tag{A37}$$

and

$$t_n|\Psi^-_{n,p,\sigma}\rangle = |t_n||\Psi^+_{n,p,\sigma}\rangle \tag{A38}$$

where t_n is the transmission amplitude for mode n. We have also introduced the state

$$|\beta\rangle = |\Psi^+_{l,p',\sigma'}\rangle, \tag{A39}$$

where the summation over β is defined as

$$\sum_{\beta} = \sum_{l}\sum_{\sigma'}\int_0^\infty dp'. \tag{A40}$$

Now let us rewrite the term $J_1^{\Rightarrow}$ as

$$J_1^{\Rightarrow} = \frac{2\pi e}{\hbar}\sum_{\alpha}\sum_{\beta}\delta_{\sigma,+1}\delta_{\sigma',+1}(f_\alpha - f_{\tilde{\alpha}})|\langle\Psi^+_{n,p,\sigma}|\hat{A}|\Psi^-_{l,p',\sigma'}\rangle|^2\delta(E_\alpha - E_\beta \pm \hbar\omega) \tag{A41}$$

where we have used the relation

$$\sum_{l,\sigma'}|\Psi^-_{l,p',\sigma'}\rangle\frac{m^*}{p'(\mathcal{E}_\alpha)}\langle\Psi^-_{l,p',\sigma'}| = \sum_{\beta}|\Psi^-_{l,p',\sigma'}\rangle\langle\Psi^-_{l,p',\sigma'}|\delta(E_\alpha - E_\beta \pm \hbar\omega). \tag{A42}$$

The total current correction J is thus

$$J = J_1^{\Rightarrow} + J_2^{\Rightarrow} = \frac{2\pi e}{\hbar}\sum_{\alpha}\sum_{\beta}\delta_{\sigma,+1}(f_\alpha - f_{\tilde{\alpha}})\delta(E_\alpha - E_\beta \pm \hbar\omega)$$
$$\times\left\{\delta_{\sigma',+1}|\langle\Psi^+_{n,p,\sigma}|\hat{A}|\Psi^-_{l,p',\sigma'}\rangle|^2 - |t_n||\langle\Psi^+_{n,p,\sigma}|\hat{A}|\Psi^+_{l,p',\sigma'}\rangle|^2\right\}. \tag{A43}$$

Every state $|\Psi\rangle$ in the above expression is either a propagating or reflecting state. We can now make a separation into propagating and reflecting states, and make use of the following relations:

$$\delta_{\sigma,+1}\delta_{\sigma',+1}|\langle\Psi^+_{n,p,\sigma}|\hat{A}|\Psi^-_{l,p',\sigma'}\rangle|^2 = \delta_{\sigma,+1}\delta_{\sigma',+1}|\langle\Psi^+_{n,p,\sigma}|\hat{A}|\Psi^+_{l,p',\sigma'}\rangle|^2 \quad \text{if } \{l,p',\sigma'\} \text{ is a propagating state,} \tag{A44}$$

$$\delta_{\sigma,+1}\delta_{\sigma',+1}|\langle\Psi^+_{n,p,\sigma}|\hat{A}|\Psi^-_{l,p',\sigma'}\rangle|^2 = \delta_{\sigma,+1}\delta_{\sigma',+1}|\langle\Psi^+_{n,p,\sigma}|\hat{A}|\Psi^+_{l,p',-\sigma}\rangle|^2 \quad \text{if } \{l,p',\sigma'\} \text{ is a reflecting state.} \tag{A45}$$

We also note that

$$\delta_{\sigma,+1}\delta_{\sigma',+1}\langle\Psi^+_{n,p,\sigma}|\hat{A}|\Psi^+_{l,p',-\sigma'}\rangle = 0 \quad \text{for propagating states,} \tag{A46}$$

$$\delta_{\sigma,+1}\delta_{\sigma',+1}\langle\Psi^+_{n,p,\sigma}|\hat{A}|\Psi^-_{l,p',\sigma'}\rangle = 0 \quad \text{for reflecting states.} \tag{A47}$$

Introducing the notations

$$|\alpha_\rightarrow\rangle = \delta_{\sigma,+1}|\Psi^+_{n,p,\sigma}\rangle \quad \text{propagating state,} \tag{A48}$$

$$|\alpha_\leftarrow\rangle = \delta_{\sigma,+1}|\Psi^+_{n,p,\sigma}\rangle \quad \text{reflecting state} \tag{A49}$$

and analogous for the state β, we can finally express the current correction J as

$$J = \frac{2\pi e}{\hbar}\sum_{\alpha}\sum_{\beta}(f_\alpha - f_{\tilde{\alpha}})\delta(E_\alpha - E_\beta \pm \hbar\omega)\left\{|\langle\beta_\rightarrow|\hat{A}|\alpha_\leftarrow\rangle|^2 - |\langle\alpha_\rightarrow|\hat{A}|\beta_\leftarrow\rangle|^2\right\}. \tag{A50}$$

Here, all states originate from the left side of the microconstriction and the arrows denote whether the states are propagating or reflecting states.

For a small applied voltage V we can make the approximation

$$f_\alpha - f_{\tilde{\alpha}} \approx eV\frac{\partial f_\alpha^0}{\partial \mu}, \tag{A51}$$

where f_α^0 is the equilibrium electron distribution function and μ is the chemical potential.

APPENDIX B

In this section we will show how the Green's function $G_0^{\pm}(E)$ can be expressed as a projection operator. This is possible only if the Green's function is situated between two operators that do not overlap each other in space. Let us denote the two operators by $\hat{\mathcal{A}}^-$ and $\hat{J}$.

As a starting point, let us rewrite the expression $\hat{\mathcal{A}}^- G_0^-(E)\hat{J}$ in x representation,

$$\begin{aligned}\langle x_1 n|\hat{\mathcal{A}}^- G_0^-(E)\hat{J}|x_2 m\rangle &= \sum_{lr}\sum_{x_3 x_4}\langle x_1 n|\hat{\mathcal{A}}^-|l x_3\rangle\langle l x_3|G_0^-(E)|r x_4\rangle\langle r x_4|\hat{J}|x_2 m\rangle \\ &= \sum_{lr}\sum_{x_3 x_4}\mathcal{A}_{nl}^-(x_1,x_3)\delta_{lr}G_0^-(x_3-x_4,E)J_{rmp}(x_4,x_2).\end{aligned} \tag{B1}$$

The Green's function can be expressed as

$$G_0^-(x_3-x_4,E) = \frac{1}{2\pi\hbar}\int_{-\infty}^{\infty} dp\frac{\exp\left(\frac{ip}{\hbar}(x_3-x_4)\right)}{E-p^2/2m^*-i\delta} = \frac{i}{\hbar}\sqrt{\frac{m^*}{2E}}\exp\left(-\frac{i\sqrt{2m^*E}}{\hbar}|x_3-x_4|\right). \tag{B2}$$

This can now be inserted into Eq. (B1). Since the two operators $\hat{\mathcal{A}}^-$ and $\hat{J}$ do not overlap in space, we always have that $x_4 > x_3$ and can therefore split the expression into two independent integrals. Introducing the wave vector $\kappa_r = \sqrt{2m^*E_r}/\hbar$ we get

$$\begin{aligned}\langle x_1 n|\hat{\mathcal{A}}^- G_0^-(E)\hat{J}|x_2 m\rangle &= \sum_{lr} 2\pi i\sqrt{\frac{m^*}{2E}}\int\frac{dx_3}{\sqrt{2\pi\hbar}}\mathcal{A}_{nl}^-(x_1,x_3)\delta_{lr}\exp(i\kappa_r x_3)\int\frac{dx_4}{\sqrt{2\pi\hbar}}\exp(-i\kappa_r x_4)J_{rm}(x_4,x_2) \\ &= \sum_{lr} 2\pi i\sqrt{\frac{m^*}{2E}}\delta_{lr}\sum_{x_3 x_4}\langle x_1 n|\hat{\mathcal{A}}^-|l x_3\rangle\langle l x_3|r\kappa_r\rangle\langle r\kappa_r|r x_4\rangle\langle r x_4|\hat{J}|x_2 m\rangle.\end{aligned} \tag{B3}$$

Finally, we can write

$$\hat{\mathcal{A}}^- G_0^-(E)\hat{J} = 2\pi i\sum_r\frac{m^*}{p_r(E)}\hat{\mathcal{A}}^-|r\kappa_r\rangle\langle r\kappa_r|\hat{J}, \tag{B4}$$

where the state $|r\kappa_r\rangle$ represents a positive momentum plane wave in the rth mode.

---

* Present address: Center for Solid State Electronics Research, Arizona State University, Tempe, AZ 85287-6206.

† Permanent address: Institute for Low Temperature Physics and Engineering, Ukrainian Academy of Sciences, Lenin Ave. 47, 310 164 Kharkov, Ukraine.

‡ Permanent address: Institute of Physics and Technology, Ukrainian Academy of Sciences, Akademicheskaya St. 1, 310 108 Kharkov, Ukraine.

[1] C. W. J. Beenakker and H. van Houten, in *Solid State Physics*, edited by H. Ehrenreich and D. Turnbull (Academic, San Diego, 1991), Vol. 44, p. 1.

[2] B. J. van Wees, H. van Houten, C. W. J. Beenakker, J. G. Williamson, L. P. Kouwenhoven, D. van der Mare, and C. T. Foxon, Phys. Rev. Lett. **60**, 848 (1988).

[3] D. A. Wharam, T. J. Thornton, R. Newbury, M. Pepper, H. Ahmed, J. E. F. Frost, D. G. Hasko, D. C. Peacock, D. A. Ritchie, and G. A. C. Jones, J. Phys. C **21**, L209 (1988).

[4] B. J. van Wees, L. P. Kouwenhoven, H. van Houten, C. W. J. Beenakker, J. E. Mooi, C. T. Foxon, and J. J. Harris, Phys. Rev. B **38**, 3625 (1988).

[5] L. I. Glazman, G. B. Lesovik, D. E. Khmelnitskii, and R. I. Shekhter, Pis'ma Zh. Eksp. Teor. Fiz. **48**, 329 (1988) [JETP Lett. **48**, 238 (1988)].

[6] L. I. Glazman and M. Jonson, Phys. Rev. B **41**, 10 686 (1990).

[7] Two articles [F. Hekking and Yu. V. Nazarov, Phys. Rev. B **44**, 11 506 (1991); **44**, 9110 (1991)] did consider electron pumping at zero bias voltage and asymmetric gate potential. Here we study the case of a symmetric gate geometry and finite bias voltage.

[8] A. Grincwajg, M. Jonson, and R. I. Shekhter, Phys. Rev. B **49**, 7557 (1994).

[9] L. Gorelik, A. Grincwajg, V. Kleiner, R. Shekhter, and M. Jonson, Phys. Rev. Lett. **73**, 2260 (1994).

[10] A. Messiah, *Quantum Mechanics* (North-Holland, Amsterdam, 1970), Chap. 21, p. 1037.

[11] Each summation over the quantum numbers α and β has the dimension of momentum, since we must integrate over the continuous momentum variable. See Eqs. (A10) and (A40) for definitions of the summations.

[12] M. Büttiker, Phys. Rev. B **41**, 7906 (1990). The exact shape of the laterally confining potential is not important in the present context. Taking the potential to be, for example, of square-well shape would lead us to qualitatively the same results. The important thing here is the existence of well-defined transverse energy levels.

[13] L. D. Landau, Phys. Z. Sowjetunion **1**, 88 (1932); L. D. Landau and E. M. Lifshitz, *Quantum Mechanics* (Pergamon, Oxford, 1987), p.185.

[14] S. Feng and Q. Hu, Phys. Rev. B **48**, 5354 (1993).

[15] R. A. Wyss, C. C. Eugster, J. A. del Alamo, and Q. Hu, Appl. Phys. Lett. **63**, 1522 (1993).

[16] Erik Kollberg (private communication).

[17] J. M. Ziman, *Elements of Advanced Quantum Theory* (Cambridge University Press, Cambridge, 1969), Chap. 4, p. 128.

[18] L. Fedichkin, V. Ryzhii, and V. V'yurkov, J. Phys. C **5**, 6091 (1993).